

# Ionospheric Estimation and Integrity Threat Detection \*

Andrew J. Hansen  
Todd Walter

Y.C. Chao  
Per Enge

Stanford University

## BIOGRAPHY

Andrew Hansen is a Ph.D candidate in the Department of Electrical Engineering at Stanford University. As a member of the GPS Laboratory at Stanford Mr. Hansen's research is focused on ionospheric estimation using tomographic inversion and integrity monitoring of WAAS ionospheric corrections.

Y.C. Chao is a Ph.D student of Aeronautics and Astronautics at Stanford University. His work currently focuses on the study of GPS dual-frequency measurement calibration, WAAS ionospheric modeling, and integrity monitoring. He received the Best Paper Award from ION GPS-93 on the subject of statistical characterization of GPS Selective Availability.

Todd Walter is a Research Associate in the Department of Aeronautics and Astronautics at Stanford University. Dr. Walter received his PhD. in 1993 from Stanford and is currently developing WAAS integrity algorithms and analyzing the availability of the WAAS signal.

Per Enge is a Research Professor in the Department of Aeronautics and Astronautics at Stanford University. Prof. Enge's research currently centers around the use of GPS as a navigation sensor for aviation. From 1986 to 1994 he was a faculty member and later an Associate Professor at Worcester Polytechnic Institute where he helped develop the use of marine radiobeacons for broadcasting DGPS data.

## ABSTRACT

A full realization of the Wide Area Augmentation System (WAAS) is intended to provide aircraft guidance throughout the en route, terminal, non-precision and precision approach phases of flight. The most demanding phase is precision approach where vertical positioning accuracy of ones of meters is necessary. Integrity

requirements ensuring safety of life specify that any vertical position errors greater than the Vertical Protection Limit be enunciated to the flight crew within six seconds. The ionosphere is the foremost impediment to such a guarantee.

Stanford, as a member of the National Satellite Test Bed (NSTB), is developing techniques for estimating the ionosphere in real-time to provide high accuracy position corrections. Paramount in the estimation process is the detection of ionospheric integrity threats. Modal decomposition of the ionosphere is the foundation of that process.

Ionospheric modes which cannot be observed by the sparse WAAS network are integrity threats if they produce large vertical position errors at the aircraft. Likewise, observable modes may threaten integrity if they either cannot be conveyed to the aircraft or decorrelate too quickly in distance or time.

We present a thought experiment for measuring the integrity of wide-area ionospheric corrections. This experiment suggests a theoretic lower bound on the ionospheric component of the vertical protection level the WAAS system can provide to the aircraft. The results of this analysis provide a point of departure for developing an integrity metric for both the WAAS system provider and aircraft on precision approach.

## INTRODUCTION

Critical to the wide area differential GPS (WADGPS) concept is the separation of the ionospheric delay from other ranging error sources [1]. The ionospheric error term is considered to be the largest positioning error source for stand alone GPS after Selective Availability (SA) [2]. Further, it is the error source with greatest uncertainty as its physics are not completely understood. In turn the correction of ionospheric error and the integrity of that correction are of utmost concern to wide-area GPS providers supporting safety-of-life

\*Supported by FAA Grant 95-6-005.

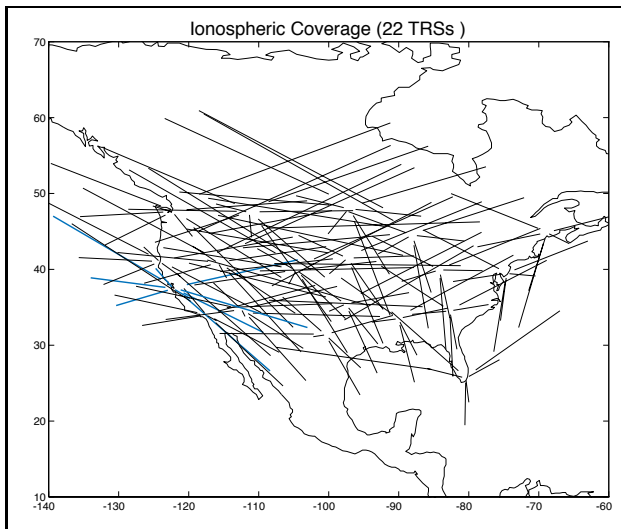


Figure 1: Ionospheric observations made by the National Satellite Testbed (NSTB) in a single epoch cover a significant portion of the ionosphere over CONUS.

applications. For Category I precision approach we consider that an integrity breach occurs when the vertical position error of an aircraft using the ionospheric correction exceeds a Vertical Protection Limit (VPL) and no warning is sent to the pilot within six seconds of the onset of the event.

In particular we analyze the FAA's Wide Area Augmentation System (WAAS). The WAAS includes a network of reference stations spatially distributed over the desired region of coverage and individual users within that region of coverage who experience unknown range delay errors. For successful operation, ionospheric observations made by the reference network must be correlated to the user's unknown delays. Below we explore the statistical relationship between the ionospheric portion of the users unknown delays and the reference network's ionospheric observations. Our objective is to measure the integrity of the ionospheric correction at a user aircraft measured in terms of vertical positioning error.

We approach our objective through a thought experiment which is framed by the following four steps: 1) Build a stochastic model of the relationship between ionospheric observations. 2) Characterize the statistical models using modal decomposition. 3) Construct integrity monitor reference chains by partitioning observations into redundant sets. 4) Compare integrity channels at the user to detect large vertical positioning error. Each step is discussed below by section. The final section presents a realization of this thought experiment.

## IONOSPHERIC DELAY OBSERVATIONS

GPS positioning is based on range measurements to a constellation of satellite vehicles (SVs) which broadcast radiowave ranging signals. Any unknown propagation delays in a user's range measurements are a direct source of positioning error. A significant source of propagation delay is the ionosphere where free electrons change the local index of refraction and thereby the velocity of a radiowave.

For single-frequency GPS users the ionospheric delay on each range measurement is unknown and hence causes positioning error. Fortunately, the dispersive nature of the ionosphere allows individual measurements of the ionosphere to be made using dual-frequency GPS receivers. The fundamental observable is the cumulative differential delay between the two frequencies over line of sight from the receiver's antenna to the SV. This differential delay represents the path integral of the electron density, or total electron content (TEC), along the line of sight ray. Measurements made at the same instant are individual in that they are sensitive to only that portion of the ionosphere which lies along that line of sight ray. That is, an observation made along a different ray results in a different cumulative differential delay. The variation in measurements is due to the spatial variation of the electron density in the ionosphere.

The WAAS ionospheric correction concept begins with a network of dual-frequency reference stations (TRSS) which make TEC measurements at each epoch. The TEC measurements are assembled by a master station (TMS) into an estimate of the ionosphere at the current epoch. That estimate is then packaged into its slot in the WAAS message stream and transmitted to single frequency users through a geostationary satellite. Received WAAS messages are decoded by a user's receiver which extracts the ionospheric estimate. The range delay errors to each SV are then corrected by subtracting the projection of the ionospheric estimate onto the line of sight ray to each SV.

The geometry of our experiment is based on the National Satellite Test Bed (NSTB), which includes 22 TRSS distributed throughout the United States and Canada. At any particular instant in time this reference network might make ionospheric observations as shown in Figure 1. The line segments radiating from each TRS are the portions of the TRS/SV rays that lie in the ionosphere from an altitude of 50-1000 kilometers. This region contains the vast majority of the free electrons in the ionosphere [3]. The TMS

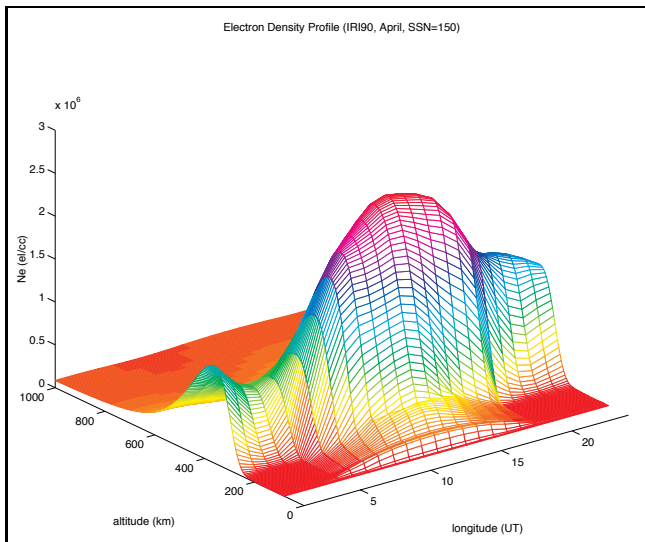


Figure 2: Electron density profiles of the ionosphere at fixed latitude can be generated by the 1990 International Reference Ionosphere (IRI90).

uses these TRS measurements of TEC to construct the ionospheric delay estimate.

In order to estimate a user's WAAS-corrected vertical position error due to the ionosphere we develop a stochastic model that captures the relationship between the TRS measurements and the user's observations. The stochastic model allows us to perform a covariance analysis on the vertical position error based on the errors in the TRS measurements. The WAAS iono correction errors are categorized into

- Error sources local to TRS and user,  $\varepsilon_n$ 
  1. Multipath,  $\varepsilon_{MP}$
  2. Residual Troposphere,  $\varepsilon_T$
  3. Receiver Thermal Noise,  $\varepsilon_N$
- Ionospheric error sources,  $d_n$ 
  1. Model Residuals,  $d_M$
  2. Finite Communications Bandwidth,  $d_{BW}$
  3. Unobserved Ionosphere,  $d_U$

The next section discusses the characterization of these error sources and outlines the covariance computation. We avoid specifying any particular ionospheric correction algorithms as our intent is to derive a metric on the integrity of any algorithm. Later reference is made to the algorithm specified in the WAAS MOPS [4] and those developed in initial WAAS implementations [5, 6].

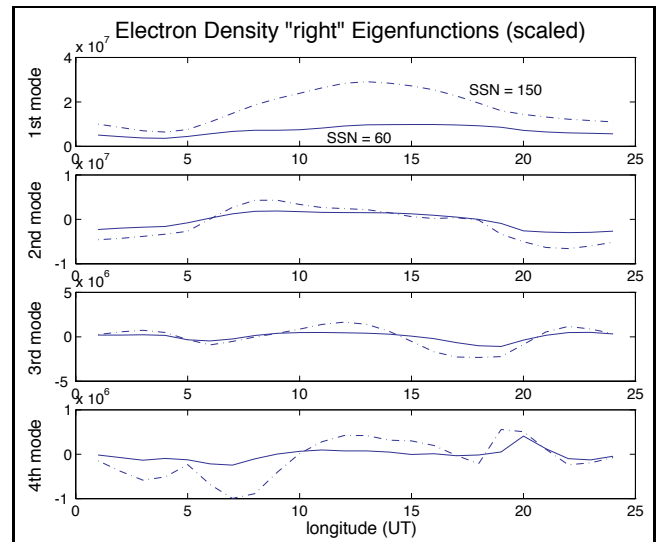


Figure 3: Spatial variation of electron density can be decomposed into modes using eigen decomposition.

## MODAL DECOMPOSITION AND STOCHASTIC MODELS

We hypothesize the ionosphere as a nominal model plus the sum of three random variables corresponding to each of the ionospheric error sources listed above,  $d_M$ ,  $d_{BW}$ , and  $d_U$ . In addition, each observation of this ionosphere is subject to the local error sources  $\varepsilon_{MP}$ ,  $\varepsilon_T$ , and  $\varepsilon_N$ . The local error sources are well modeled as elevation dependent, spatially uncorrelated, zero-mean, Gaussian random variables [2].

Each of the ionospheric error sources have some finite power and are spatially correlated between individual observations. Assuming these error sources are also Gaussian, we need only find the power (variance) and decorrelation function of each term to complete our stochastic model.

Modal decomposition is central to the characterization of stochastic models for the three ionospheric error sources in that it is powerful enough to work in the electron density domain and yet flexible enough to accommodate any ionospheric correction algorithm. This is a significant advantage not only because of its ability to analyze different algorithms but also because it can be used in the formulation of an integrity metric in the WAAS receiver. Modal decomposition is closely related to computerized ionospheric tomography (CIT) via generalized inverse theory [7] and its utility here is as follows.

Consider the ionosphere as a series of modes, each mode being the product of basis functions in latitude,

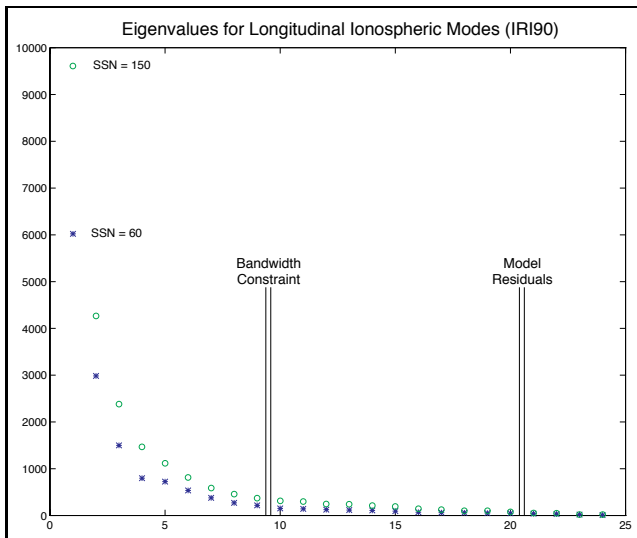


Figure 4: Electron density eigenfunctions have associated eigenvalues which represent the strength of each mode.

longitude, and altitude. By employing modal (eigen) decomposition of the electron density in the ionosphere we can determine the spatial variation in each mode, i.e. its eigenfunction, and the power in that mode, i.e. its eigenvalue. The characterization of the error sources is then the process of assigning modes to error sources. The power in a particular error source is the sum of the modal eigenvalues assigned to that error and the decorrelation function is the regression of the spatial variation in the associated eigenfunctions.

An example scenario is depicted in Figures 2, 3 and 4 where the empirical ionospheric model IRI90 [8] is used to generate electron density profiles in latitude, longitude and altitude at various seasons and sun spot numbers (SSNs). Figure 2 shows the electron density profile at a fixed latitude as a function of altitude and longitude in April with SSN equal to 150.

The basis functions of the first four modes are shown in Figure 3. Note that they are ranked by magnitude and modes with greater spatial variation have lower power since the IRI90 model is smooth. The corresponding eigenvalue plot is shown in Figure 4 where we have assigned modes to respective error sources. The group of modes lying to the left of the first double bar capture the correctable ionospheric delay that can be transmitted to and used by the aircraft considering communication bandwidth limitations. The modes lying between the two sets of double bars capture the portion of ionospheric delay the TMS can estimate from the TRS observations but cannot transmit to the user because of finite bandwidth. These modes correspond

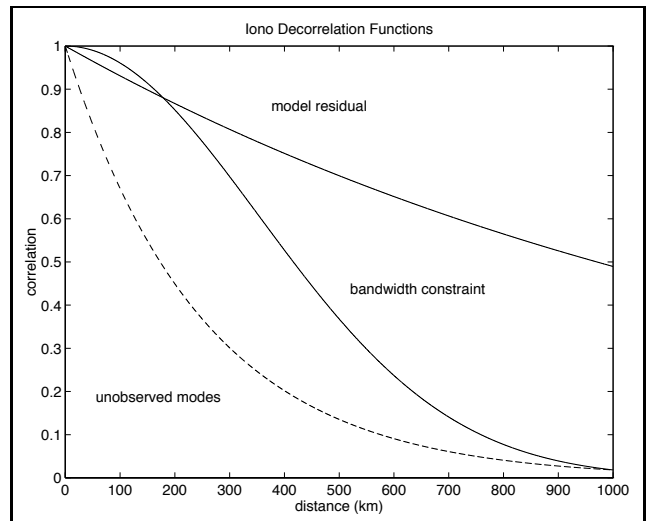


Figure 5: Each error source in the WAAS ionospheric correction has a unique decorrelation function.

to the  $d_{BW}$  error source. Finally, the modes to the right of the second double bar capture the algorithmic errors in the ionospheric delay estimation and correspond to the  $d_M$  error source.

Of particular importance is the lack of modes assigned to the unobserved ionosphere,  $d_U$ , which by definition cannot be observed by the WAAS reference network. The power in this term has no clear relation to the other error sources and is not well known. It is necessary therefore to parameterize our covariance analysis of the user's vertical position error over the power in the unobserved ionospheric modes. On the other hand the decorrelation function associated with  $d_U$  does relate to the first two error sources. For the WAAS to provide a viable ionospheric correction to all users in the region of coverage,  $d_U$  must decorrelate "faster" than the model or bandwidth constraint errors.

A basis of eigenfunctions and eigenvalues is developed by applying modal decomposition repeatedly over electron density profiles in all three dimensions. To simplify the determination of the decorrelation functions for our thought experiment the eigenfunctions were regressed as a batch over all three dimensions at once.

The resulting stochastic models for the three error sources are spatially correlated Gaussians characterized by

1. Model Residuals,  $d_M \sim \mathcal{N}(0, \sigma_M^2, f_M(|r|))$
2. Finite Bandwidth,  $d_{BW} \sim \mathcal{N}(0, \sigma_{BW}^2, f_{BW}(|r|))$
3. Unobserved Ionosphere,  $d_U \sim \mathcal{N}(0, \sigma_U^2, f_U(|r|))$

where the decorrelation functions  $f_M$ ,  $f_{BW}$ , and  $f_U$ , are shown in Figure 5.

The expression of the decorrelation as a scalar function of distance is a simplification for computational efficiency, and as noted decreases the vertical protection error. This is acceptable only in this thought experiment where we are searching for a lower bound. Real-time integrity monitoring must estimate these decorrelation functions in order to make an accurate measurement of the integrity of the WAAS iono correction.

The user's vertical position error is then the projection of the covariance between user observations and TRS observations through the user's weighted navigation matrix. Each observation is a function of only the six Gaussian error sources,  $d_M, d_{BW}, d_U, \varepsilon_{MP}, \varepsilon_T, \varepsilon_R$ , so that the covariance computation can be carried out using only the first two moments of each random variable. The result of the covariance computation is a Minimum Mean Square Error (MMSE) estimate,  $\hat{z}$ , of the true vertical position error,  $z$ .

## INTEGRITY MONITORING

The key to monitoring the integrity of the WAAS iono correction is redundancy. We exploit the large number of ionospheric measurements made by the WAAS network at any one instant by partitioning the TRS observations into two or more reference chains. If each chain has nearly equal ability to estimate the user's vertical position error, the estimates,  $\hat{z}_i$  can be compared against a protection threshold that is based on the acceptable false alarm rate under nominal ionospheric conditions. An alarm is raised when a given estimate exceeds the threshold.

Two common forms for partitioning the TRS observations are to either divide all the measurements into sets, each having null intersection with the rest, or index overlapping sets which share all but one observation. In each case the deleted observations must have strong correlation with the true vertical position error,  $z$ , for the estimators to be meaningful. We chose to implement the second form of integrity monitor partitioning in the current experiment. This closely resembles the RAIM methodology described in [9].

Taking the difference,  $z - \hat{z}_i$ , the vector of position error residuals,  $\underline{\varepsilon}$ , from all reference chains can be transformed into a vector of orthogonal accuracy and integrity estimates,  $[\varepsilon_P, \varepsilon_{I1}, \varepsilon_{I2}, \dots]^T$ . Supposing  $J$  chains, this transformation has the following properties:

1. The first transformed variable is the weighted average of the position error estimates and represents the position accuracy.

2. The remaining  $J - 1$  variables are the error estimators residuals with respect to the true position error and represent the correction integrity.
3. The integrity variables are functions of the TRS observations only.
4. The accuracy and integrity statistics are uncorrelated.

The linear transformation from a vector of position error estimates into a vector of uncorrelated accuracy and integrity estimates is in fact just a whitening matrix.

At any epoch the existence of independent accuracy and integrity statistics allows us to compute the probability that the vertical position error exceeds the VPL and none of the integrity monitors raises an alarm. This condition is an integrity breach and in the FAA's lexicon is called the probability of hazardous misleading information,  $\text{Pr}(\text{HMI})$ . It is this quantity we seek to measure with our integrity metric.

## INTEGRITY PROCESSING

Figure 6 is a graphical rendition of the integrity monitoring process for a single epoch. Integrity processing begins at each epoch with the partitioning of TRS observations into reference chains. As mentioned above it is critical that the observation deleted from a reference chain be highly correlated with the vertical position error at the aircraft. For the stochastic models constructed in the MODAL DECOMPOSITION section, it is obvious that the measurements geometrically nearest the user's observations have the highest correlation to the user's range measurement errors.

To avoid the inordinate number of reference chains produced by dropping one TRS observation from the set of all observations, we fix the number of reference chains,  $J$ , to be the maximum number of SVs in view of the the WAAS receiver. Each reference chain drops the measurement nearest the  $i^{\text{th}}$  user observation. If the same TRS measurement is dropped in more than one chain the next closest measurement to the  $i^{\text{th}}$  user observation is dropped to ensure uniqueness.

The notion of a scalar distance between observations warrants clarification. The simplification of the decorrelation function into a scalar function of distance requires the distance between observations be approximated in some way. The distance approximation we have implemented returns the ten point average of the true distance between the line of sight rays. Partition-

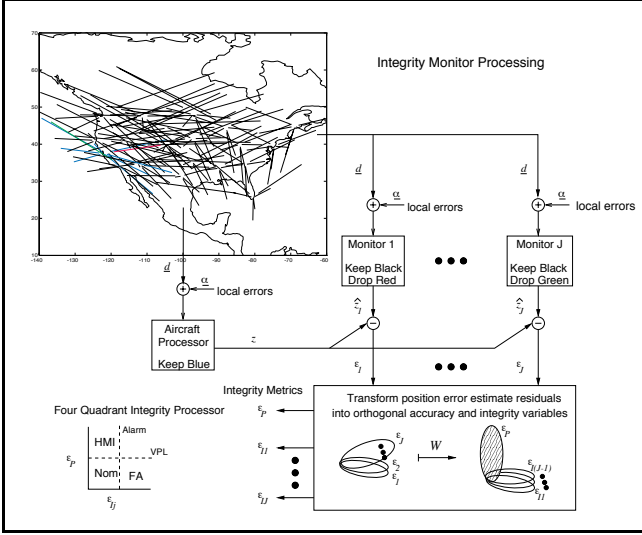


Figure 6: The integrity monitor process is the combination of estimating the vertical position error then transforming those estimates into accuracy and integrity statistics.

ing of reference chains is insensitive to this approximation as only extreme corner cases will change the TRS measurement to be dropped. Even then the gradient on the decorrelation functions is small enough that the correlation coefficients of two such observations are indistinguishable.

After dividing the TRS observations into reference chains, the covariance matrix between the user's observation and each reference chain is computed. The resulting MMSE estimate,  $\hat{z}_i$ , from each reference chain is then subtracted from the true position error,  $z$ , at the aircraft to form the residual vector,  $\underline{\varepsilon}$ .

$$\begin{bmatrix} \varepsilon_1 \\ \varepsilon_2 \\ \varepsilon_3 \\ \vdots \\ \varepsilon_J \end{bmatrix} = z - \begin{bmatrix} \hat{z}_1 \\ \hat{z}_2 \\ \hat{z}_3 \\ \vdots \\ \hat{z}_J \end{bmatrix}$$

This residual vector is transformed into the vector of accuracy and integrity estimates,  $[\varepsilon_P, \varepsilon_{I1}, \dots, \varepsilon_{IJ}]^T$ , by simple matrix multiplication with the whitening matrix,  $W$ .

$$\begin{bmatrix} \varepsilon_P \\ \varepsilon_{I1} \\ \varepsilon_{I2} \\ \vdots \\ \varepsilon_{I(J-1)} \end{bmatrix} = W \cdot \begin{bmatrix} \varepsilon_1 \\ \varepsilon_2 \\ \varepsilon_3 \\ \vdots \\ \varepsilon_J \end{bmatrix}$$

As mentioned in the INTEGRITY MONITORING section, the linear transformation,  $W$ , maps the

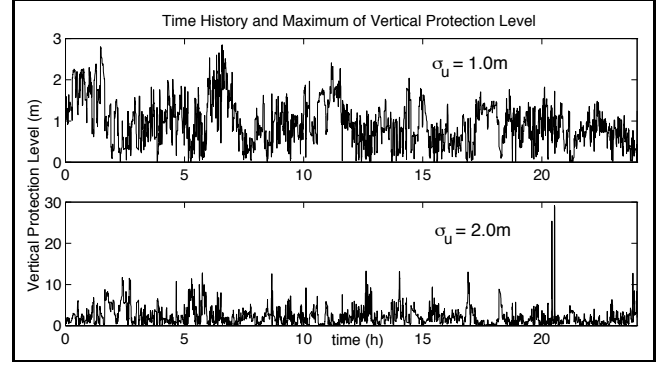


Figure 7: The WAAS ionospheric correction integrity metric can be used to compute the vertical protection limit provided by the WAAS iono correction.

weighted average of the residuals  $\varepsilon_i$  into  $\varepsilon_P$ . The remaining  $J - 1$  rows of the whitening matrix map the differences between the residuals into the integrity statistics,  $[\varepsilon_{I1}, \varepsilon_{I2}, \dots, \varepsilon_{I(J-1)}]^T$ ,

The integrity measurement is carried out by computing the  $\text{Pr}(\text{HMI})$ , that is the joint probability that the accuracy estimate,  $\varepsilon_P$  exceeds the VPL while none of the integrity estimates,  $\varepsilon_{Ij}$  exceed the alarm threshold. The alarm threshold is set by the continuity constraint,  $\text{Pr}(\text{FA})$ , which is the probability of false alarm under normal operation.

## THEORETIC BOUND ON VERTICAL PROTECTION LEVEL

By recasting the integrity measurement with a fixed probabilities of integrity breach,  $\text{Pr}(\text{HMI})$ , and continuity failure,  $\text{Pr}(\text{FA})$ , we can explore the vertical protection level provided by the WAAS iono correction. In particular we are interested in the lower bound an optimal WAAS correction process can achieve given a fixed reference network geometry. Here we consider the optimal WAAS iono correction to be one with no modeling errors and unlimited bandwidth, which translates into the removal of the first two error sources,  $d_M$  and  $d_{BW}$ .

The two plots in Figure 7 trace the time history of the vertical protection level a simulated optimal WAAS iono correction could protect with an integrity of 99.99999% [ $\text{Pr}(\text{HMI}) = 10^{-7}$ ] given an unobserved ionosphere with power  $\sigma_U$ . The conditions of this experiment were as follows

- Single user located at SFO
- Reference network of 21 TRSs
- $5^\circ$  TRS elevation mask,  $7\frac{1}{2}^\circ$  user elevation mask
- Full GPS constellation of 24 SVs, no GEOs

- Continuity constraint of  $\Pr(\text{FA}) = 10^{-4}$

Recall that we have parameterized the vertical positioning error over  $\sigma_U$  so that each time history is corresponds to one value of  $\sigma_U$ . The top graph is the lower bound on the vertical protection level for  $\sigma_U = 1.0\text{m}$  and the bottom graph is the lower bound for  $\sigma_U = 2.0\text{m}$ . Notice that the protection level of the lower power ionosphere is bounded by 3.0m and is relatively insensitive to the geometry of the GPS constellation. On the contrary, the protection level of the higher power ionosphere is very spikey and barely contained by 30.0m around hour 20.

Parameterizing  $\sigma_U$  over the interval [0.1,2.0] meters, it was clear for  $\sigma_U$  about 1.0m and below the vertical protection level is dominated by the local errors on the ionospheric observations and hovers around a protection level floor of 3.0m. However just above 1.0m the unobserved ionospheric modes begin to dominate the local errors and the maximum protection level over the 24 hour period begins to grow rapidly.

## CONCLUSIONS

The integrity metric derived here is a direct measure of the impact algorithmic errors, finite bandwidth, and reference station placement have on the WAAS ionospheric correction process in terms of the user's vertical protection level. This integrity metric combines modal decomposition of error sources with a partitioning of WAAS ionospheric measurements to form a set of integrity monitors for the user.

This integrity monitoring process may be sensitive to the scalar approximation to the decorrelation function and a more sophisticated modal decomposition is underway.

In the future we plan to use the NSTB to build up an archive of observation data. This archive can be used to refine the empirical basis functions currently drawn from IRI90. In addition, passing live observations through the integrity process should identify areas for improvement. Our integrity metric can also be a useful tool for studying the possible benefits of adding GLONASS observations to reduce the unobserved regions of the ionosphere. Likewise, it can quantify the benefit of turning off SA which effectively increases the WAAS communication bandwidth.

## ACKNOWLEDGMENTS

The authors wish to thank Dr. Boris Pervan and Dr. Sam Pullen at Stanford University for the many helpful insights offered from their work in LAAS integrity algorithms. We also gratefully acknowledge the FAA Technical Center and Satellite Navigation Office for sponsoring our WAAS research through the NSTB.

## REFERENCES

- [1] C. Kee, B. W. Parkinson, and P. Axelrad, "Wide area differential GPS," *Navigation*, vol. 38, no. 2, 1991.
- [2] P. Enge, T. Walter, S. Pullen, C. Kee, Y.-C. Chao, and Y.-J. Tsai, "Wide area augmentation of the the global positioning system," *Proceedings of the IEEE*, vol. 84, no. 8, pp. 1063–1088, 1996.
- [3] J. Hargreaves, *The Solar–Terrestrial Environment*. Cambridge: Cambridge University Press, 1992.
- [4] RTCA Special Committee 159, *Minimum Operational Performance Standards for Global Positioning System/Wide Area Augmentation System Airborne Equipment*, RTCA/CO-229, November 1996.
- [5] Y.-C. Chao, S. Pullen, P. K. Enge, and B. W. Parkinson, "Study of WAAS ionospheric integrity," *Proceedings of the Institute of Navigation GPS-96*, pp. 781–788, September 1996.
- [6] A. Draganov, T. Cashin, and J. Murray, "An ionospheric correction algorithm for WAAS and initial test results," *Proceedings of the Institute of Navigation GPS-96*, pp. 789–797, September 1996.
- [7] E. Fremouw, J. Secan, R. Bussey, and B. Howe, "A status report on applying discrete inverse theory to ionospheric tomography," *International Journal of Imaging Systems and Technology*, vol. 5, pp. 97–105, 1994.
- [8] D. Bilitza, K. Rawer, L. Bossy, and T. Gulyaeva, "International reference ionosphere—past, present, future," *Advances in Space Research*, vol. 13, no. 3, pp. 3–23, 1993.
- [9] R. Brown, *Autonomous Integrity Monitoring, GPS Theory and Applications*. Washington, D.C.: AIAA, 1996. eds. Parkinson, Spilker, Axelrad, and Enge.